IEEE Access
Multidisciplinary ⋮ Rapid Review ⋮ Open Access Journal

Received December 7, 2019, accepted December 22, 2019, date of publication December 25, 2019, date of current version January 3, 2020.

Digital Object Identifier 10.1109/ACCESS.2019.2962141

Design of a Super Wide Band Antenna and Measure of Ambient RF Density in Urban Area

LINGSHENG YANG[1], (Member, IEEE), DAN ZHANG[2], (Member, IEEE), XIAOLEI ZHU[1], AND YAJIE LI[3]

[1]Jiangsu Key Laboratory of Meteorological Observation and Information Processing, Research Center of Applied Electromagnetics, Nanjing University of Information Science and Technology, Nanjing 210044, China
[2]College of Information Science and Technology, Nanjing Forestry University, Nanjing 210037, China
[3]Zhongda Hospital, Southeast University, Nanjing 210009, China

Corresponding author: Yajie Li (withlove1982@163.com)

This work was supported in part by the Special Funds for Basic Scientific Research of Southeast University under Grant 2242019K40267, in part by the Priority Academic Program Development of Jiangsu Higher Education Institutions (PAPD), and in part by the Kunshan & Nanjing University of Information Science and Technology (NUIST) Intelligent Sensor Research Center Project.

ABSTRACT A compact Super Wide band (SWB) antenna fed by coplanar waveguide (CPW) is proposed in this paper. The size of the antenna is $140 \times 100mm^2$ ($0.16\lambda \times 0.12\lambda$). The antenna originates from 3D volcano smoke antenna, and consists of a prolonged radiation patch and a symmetrical ground. Both the patch and ground were designed as smoothing structure, which can improve the impedance matching through a wide band. The simulated and measured bandwidth show that the antenna has a well-matched impedance bandwidth from 400MHz to higher than 20GHz under VSWR = 2 criterion, and the bandwidth ratio is greater than 50:1. The gain, efficiency and radiation pattern were all measured, and the maximum gain and efficiency are 6.3dBi and 96%, respectively. The antenna was also used to measure the ambient radiation frequency (RF) density in an urban area of Nanjing in China, which on the other hand proves the efficiency of this design.

INDEX TERMS SWB antenna, coplanar waveguide, bandwidth ratio, ambient radiation frequency density.

I. INTRODUCTION

With the rapid development of wireless communication technologies, many wireless communication systems have been developed, such as DTV (400-800MHz), GSM850 (824–894MHz), GSM900 (880–960MHz), GSM1800/1900, GPS (1.57-1.58GHz), WLAN (2.4GHz/5.8GHz), 4G LTE bands (from 452.5-3800MHz), newly licensed sub-5G bands (3.3-4.2GHz and 4.4-5.0GHz), and UWB (3.1-10.6GHz). The current antenna design trends to support these multistandard wireless communication systems by a single antenna element. Meanwhile, because of the highly limited space available for antenna installation in communication devices, a compact wideband antenna with low profile is preferred. Since Rumsey et al. [1] designed a series of broadband antennas with a ratio bandwidth greater than 10:1 from the late 1950s to early 1960s, and defined them as Super Wideband (SWB) antennas, SWB antennas have attracted a lot of attention from both the academy and industry due to their advantages of large bandwidth, large channel capacity, and high time precision [2].

Many SWB antenna designs have been reported recently [3]–[16]. Among them, antennas with fractal structure are widely used [3]–[5]. Although they are a little bit complicated in design, they can perform wideband performances with low profile. In [3], iterative octagon microstrip antenna was proposed, the antenna can cover 10GHz-50GHz with a dimension of $60 \times 60mm^2$. A SWB fractal antenna based on circular-hexagonal geometry was proposed in [4], radial arrow shaped fractal slots forms the path of surface currents and lead to a super wide band from 2.18GHz to 20GHz. A printed fractal monopole antenna is presented for SWB applications was presented in [5]. By applying star-triangular as the fractal generator, the proposed antenna obtained a bandwidth of 29 GHz (1GHz-30 GHz).

Besides fractal geometry, planar monopole antennas are good candidates for super wideband applications [6]–[12]. By carefully designing appropriate shapes of the radiation element and the truncated ground, wideband performances can be realized. In [6], a planar monopole consists of a

The associate editor coordinating the review of this manuscript and approving it for publication was Lei Zhao.

radiating patch (made of one half-disc and one half-ellipse), a corner-rounded ground plane, and a tapered microstrip feeder was proposed. The antenna has a ratio bandwidth more than 25:1 (VSWR<2). An egg-shaped monopole was presented in [7], a fractal-complementary slot was embedded into the asymmetrical ground plane, and the proposed antenna was able to perform well from 1.44GHz to 18.8 GHz. In [8], the planar monopole consists of a tapered radiating patch and a rectangular truncated ground, and can operate over a bandwidth of 2.5GHz-80GHz with $S_{11} < -10dB$. A trapezoidal ground plane with top rounded corners can help the planar monopole to obtain a better impedance match from 0.72GHz to 25GHz [9]. Similar like other planar monopole designs, the gap between the radiation patch and the ground plays an essential role in wideband design. A miniaturized asymmetrical printed SWB antenna evolved from standard symmetrical elliptical printed monopole was proposed in [10], the antenna has 2:1 VSWR bandwidth ranges from 0.47GHz to 25GHz. With antenna structures similar like [10], new feed networks (L-shaped branch or semi-ring feed interface) were applied in [11] and [12], respectively to enhance the bandwidth, and the 2:1 VSWR bandwidth are from 1.05GHz to 32.7GHz and 1.08GHz to 27.4GHz accordingly.

Metamaterials and metasurfaces can also be used to obtain super wideband performances. In [13], L-shaped slits and inductive spirals were used, without increasing the aperture of the antenna, a 0.48-6.5GHz bandwidth was achieved. Meander-line slots and four double split-ring resonators were applied in [14], the bandwidth was enhanced, and can cover 115MHz to 2.9GHz.

Compared to the aforementioned antenna designs, CPW-fed planar antenna has only one-layer structure, and is easier to fabricate and integrate with printed circuits [15]. In [16], two operating bands of 2.07GHz-2.22 GHz and 3.5GHz-50GHz can be achieved by designing the antenna with an L-shaped structure and applying a semicircle notch into the ground plane. The printed SWB antenna proposed in [17] evolved from the discone antenna, with a compact size of $0.19\lambda \times 0.16\lambda$, a ratio impedance bandwidth of 21.6:1 can be achieved. A planar SWB loop antenna [18] with asymmetric CPW feed was introduced, and a ratio bandwidth of more than 41.7:1 with a reflection coefficients of -10dB was obtained.

In this paper, a compact symmetrical CPW-fed SWB antenna is proposed. The antenna's origin is a conventional 3D volcano smoke antenna. Both the simulated and measured results show that the antenna has a wide and well matched impedance bandwidth from 400MHz to higher than 20GHz, so the antenna can support a variety of communication systems (including all the aforementioned wireless systems). The good radiation performances of the antenna can be further verified by testing the antenna both in anechoic chamber and real environment. The rest of the paper is organized as follows: Section II describes the design of the antenna. The measured results and discussions are presented in Section III. The fabricated antenna is used to measure the ambient RF power density in an urban area in Nanjing, and the results are analyzed in Section IV. Finally, in Section V, conclusion is made.

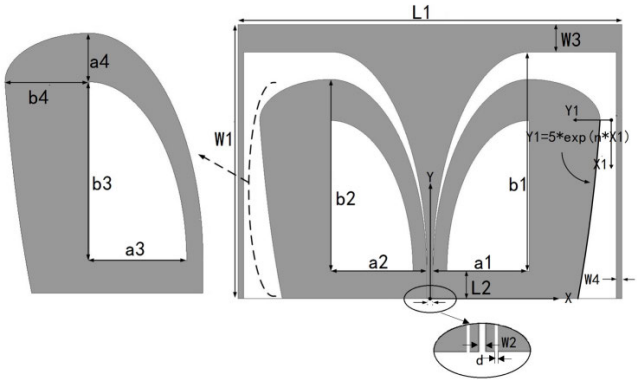

FIGURE 1. Configuration of the proposed SWB antenna.

II. ANTENNA DESIGN

The configuration of the proposed SWB antenna is shown in Fig.1. The antenna is located on the top of a 1mm thick FR4 substrate (relative permittivity of 4.4 and loss tangent of 0.02) with a size of $140mm \times 100mm(L_1 \times W_1)$. The antenna is fed by using a coplanar waveguide (CPW) structure. The width of the feed line is set as W_2, and the gap between the feed line and the ground is d_1. The parameters of the feed structure is optimized, so 50Ω impedance matching can be fulfilled through the whole band.

The symmetrical antenna consists of a radiation patch and specially shaped ground. As mentioned in [19], strong localized diffractions may be caused by abrupt discontinuities, and in turn will narrow down the bandwidth. So for both the radiation patch and the ground plane, smooth connection (especially among feed structure) is necessary.

The edge of the radiating patch connected to the feed structure is designed as a quarter ellipse with a long semi-axis of b_1, and a short semi-axis of a_1. Then both sides of the patch are extended by two rectangular segments with widths W_3 and W_4, which can increase the current path length. In fact, according to equation (1), the prolonged current path length (including a quarter of the perimeter of the ellipse together with the length of the two rectangular segments) is 214mm, which is about 1/2 wavelength of the lowest operating frequency ($\lambda = 456.4mm@400MHz$).

$$\lambda = \frac{c}{\sqrt{\varepsilon_{eff}} f} \tag{1}$$

where

c = the speed of light and $\varepsilon_{eff} = \frac{\varepsilon_r + 1}{2}$

The outside edge for either side of the ground is formed by two quarter-ellipses and an exponential curve. The long semi-axis and short semi-axis of the ellipse connected with the feed structure are b2 and a2. The gap between the two ellipses (the radiation patch and the ground) becomes a flared

TABLE 1. Optimized parameters of the SWB antenna (Unit: mm).

Parameters	Value	Parameters	Value
L_1	140	a_3	30
L_2	10	a_4	15
W_1	100	b_1	80
W_2	2	b_2	70
W_3	10	b_3	55
W_4	2	b_4	25
a_1	35	d_1	0.2
a_2	35	n	15

slot which can be treated as a broadband impedance transformer. So good impedance matching in wide band can be fulfilled, and which ensures the SWB performances. While for the ellipse at the upper corner of the ground, the long and short semi-axes are b4 and a4. The exponential curve is established in a coordinate system where the origin of coordinates in the $X_1O_1Y_1$ plane is $O_1(\frac{W_2}{2} + d_1 + a_2 + a_4 + m, L_3 + b_4)$, and the two ends of the curve are located on the elliptic vertex at the upper corner and the lower edge of the antenna, respectively. The function is finally defined as $y_1 = 5 \times e^{nx_1}$.

Two quarter-ellipses with a long semi-axis of b_3 and a short semi-axis of a_3 are symmetrically notched in the ground plane. These changes can help further improve the impedance matching.

The antenna was simulated by using ANSYS high-frequency structure simulator (HFSS) software, and the optimized parameters of the proposed SWB antenna are listed in Table 1.

III. RESULTS AND DISCUSSION

Since the antenna is single-layer structure, it is easy to fabricate. Fig.2 exhibits the photograph of the antenna. Considering the frequency limitation of the SMA connector and the cost of time for simulation, we only test the antenna in the frequency range up to 20GHz for both simulated and measured results.

The impedance bandwidth was measured by using Agilent Model 85058E vector network analyzer. Fig.3 shows the comparison between simulated and measured impedance bandwidth. For both results, good impedance matching (less than -10dB) can be fulfilled through the 0.4-20GHz band. The differences of reflection coefficients level are mainly cause by fabrication error and the differences of dielectric characteristics between real material and simulation ones. It can also

FIGURE 2. Photo of the fabricated antenna.

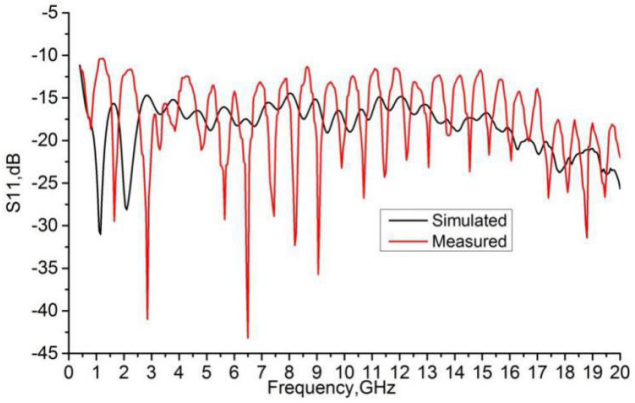

FIGURE 3. Antenna measurement and simulation S11.

be noted that even at 20GHz, the measured S_{11} value of the antenna is still lower than -10dB, which means the actual bandwidth ratio is larger than 50:1

When the total size and the overall structure has been determined, the change of one parameter affects but will not change the well impedance matching for frequency band higher than 3.2GHz. So for parameters study, we only consider the frequency band from 0.4-3.2GHz.

The length of the short semi-axis a_1 in Fig.1 has an influence on the impedance matching of the antenna in the entire band. For frequency lower than 3.2GHz, as shown in Fig.4, when $a_1 = 15$mm, except for 1.6-2.4GHz, the S_{11} is larger than -10dB, which indicates that the antenna is not well matched. With the increase of a_1, the impedance matching keep on improving, and a new resonance frequency point around 1.1GHz occurs.

How the shape of the ground can affect the impedance matching is also discussed. The influence of the change of a_2 on S_{11} is analyzed in Fig.5. With the increase of a_2, the impedance matching around 1.1GHz improved, and the lower band of the SWB antenna occurs.

As shown in Fig.6, the parameter n for the exponential curve $y_1 = 5 \times e^{nx_1}$ mainly affects part of the ground which

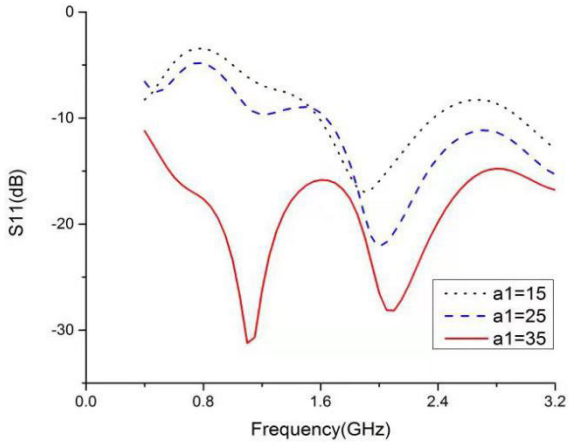

FIGURE 4. Effect of a1 on antenna S_{11}.

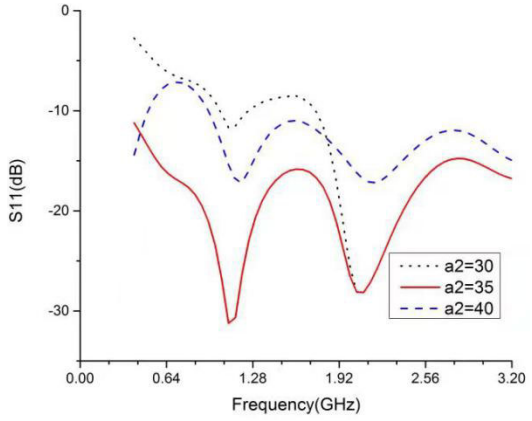

FIGURE 5. Effect of a_2 on antenna S_{11}.

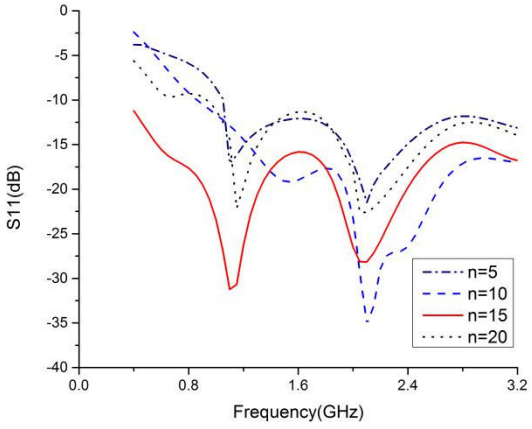

FIGURE 6. Effect of n on antenna S_{11}.

is not so close to the feed section. When $n = 5$, the curvature of the function is low, It can be seen that the impedance matching of the antenna is poor in the frequency band lower than 1.1GHz. As n increase, the impedance matching improved. However, when $n > 15$, the impedance matching is deteriorated.

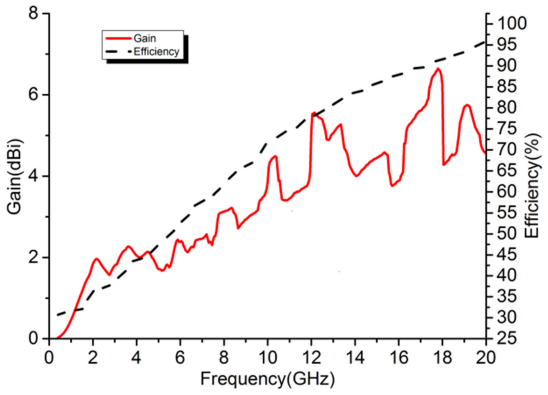

FIGURE 7. Measured antenna gain and radiation efficiency.

TABLE 2. Comparison of the proposed antenna with other published SWB antenna designs.

Designs	Size, mm^2 / λ^2	Bandwith (GHz)	Ratio of Bandwith
[4]	45×33 / 0.33×0.23	2.18-44.5	20.4:1
[6]	150×150 / 0.32×0.32	0.64-16	25:1
[7]	77×35 / 0.37×0.168	1.44-18.8	12:1
[8]	40×30 / 0.33×0.25	2.8-80	32:1
[9]	150×150 / 0.36×0.36	0.72-25	34:1
[13]	23×17 / 0.077×0.057	0.48-6.5	13.5:1
[14]	48.32×43.72 / 0.235×0.211	0.115-2.9	25.2:1
[17]	140×140 / 0.19×0.19	0.41-8.86	21.6:1
This work	140×100 / 0.16×0.12	0.4-20	50:1

The measured gain and radiation efficiency are plotted in Fig.7. We can see that, the gain and efficiency generally increase with the increase of frequency. The peak gain is 6.3dBi through the whole band, while the efficiency changes from 30% to 96%.

The measured radiation patterns of the antenna at 400MHz, 900MHz, 1.8GHz, 2.4GHz, 5.8GHz, 10GHz and 15GHz are shown in Fig.8. We can see that the antenna has quasi-omnidirectional performances at lower operating frequency, especially at lower than 5GHz band. Also, eight shaped radiation pattern can be observed for E-plane at the lower frequency band, and more radiation nulls occur for higher frequency.

The proposed SWB antenna has been compared with other recently published SWB antennas. As summarized in Table 2, we can see that our design has a wider bandwidth (larger ratio of bandwidth) than other SWB antennas, while only need a small size.

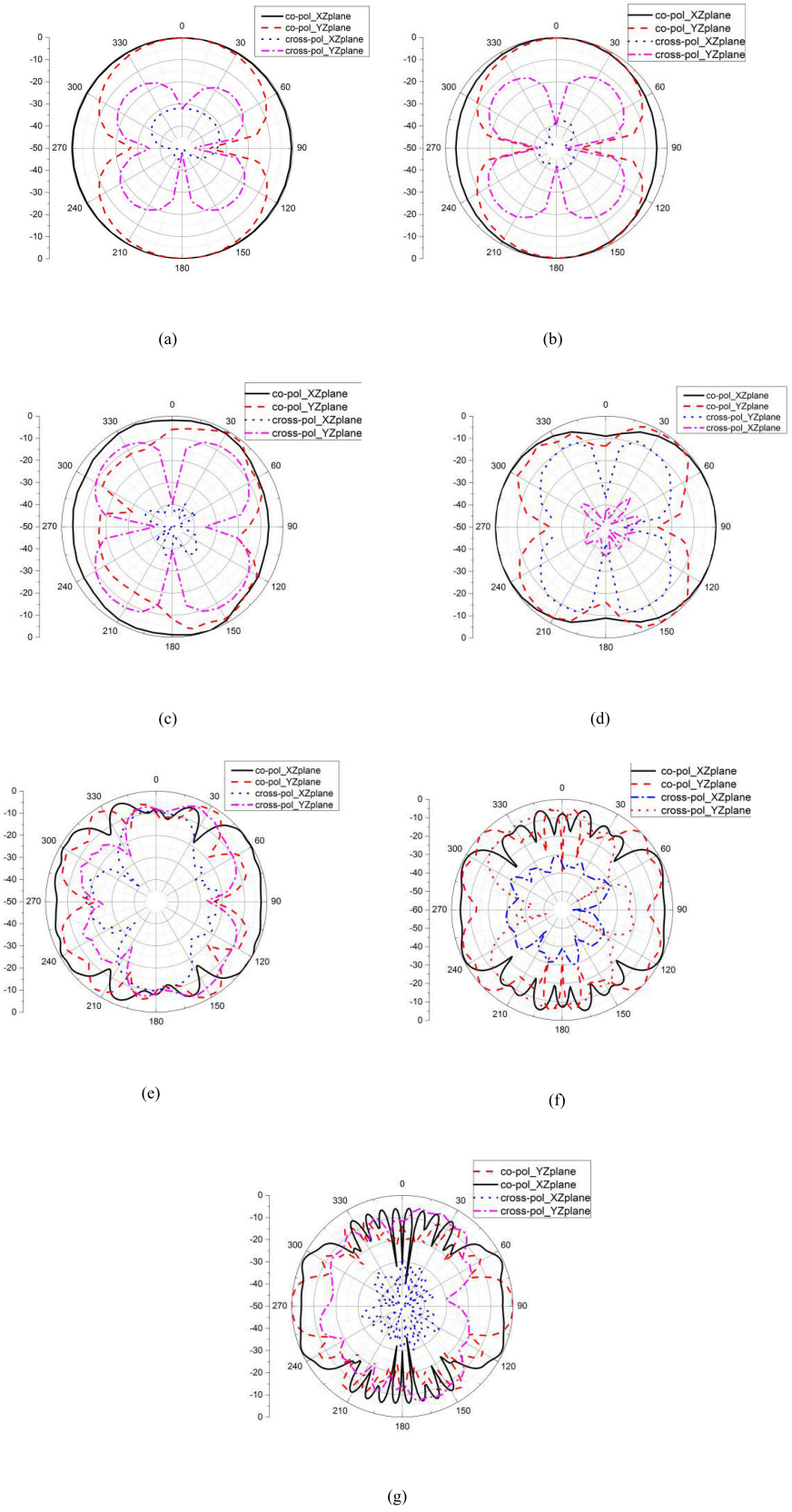

FIGURE 8. Measured radiation patterns, (a) 400MHz (b) 900MHz, (c) 1.8GHz, (d) 2.4GHz, (e) 5.8GHz, (f) 10GHz, (g) 15GHz.

FIGURE 9. RF power density measurement.

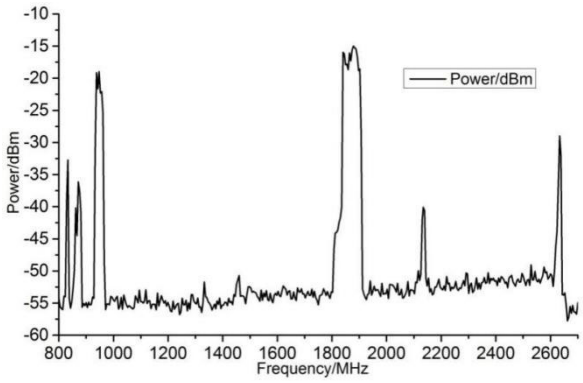

FIGURE 10. Measured RF power density as a function of frequency.

IV. MEASURE OF AMBIENT RF POWER DENSITY

On the basis of the measured results, the proposed SWB antenna can obtain well impedance matching through 0.4-20GHz with acceptable radiation performances, so it can work for almost all the currently existing wireless standards in cities, such as DTV, GSM, DCS, UMTS, 4G LTE, WLAN (2.4/5.8GHz), and so on. In this section, instead of a broadband discone antenna[20], we connected the SWB antenna to a portable spectrum analyzer (Agilent N9918A), and measured the RF power density in Gulou District, urban area in Nanjing, a city in East China (Fig.9). According to the wireless systems on service in Nanjing, the analyzer was configured with a start and stop frequency of 0.8 and 2.7 GHz, respectively, and the resolution bandwidth was fixed as 200 kHz.

The test site is on the roof of a primary school, close to a base station tower which is shared by the three major telecommunications operators in China (China Mobile, China Unicom and China Telecom). According to the measured results (Fig.10), the wireless systems in service are as follows: China Mobile GSM (935-954MHz), China Unicom GSM (954-960MHz), China Unicom DCS (1830-1850MHz), China Unicom FDD-LTE (1850-1860MHz), China Telecom

TABLE 3. Single frequency point RF energy data in the China Unicom FDD-LTE band.

Frequency (MHz)	$P_s(f)$ ($\mu W/cm^2$)	Frequency (MHz)	$P_s(f)$ ($\mu W/cm^2$)
1850	0.063555585	1855.2	0.073368967
1850.2	0.057940482	1855.4	0.030247136
1850.4	0.068353499	1855.6	0.069250599
1850.6	0.080727164	1855.8	0.060684609
1850.8	0.05391621	1856	0.037958237
1851	0.057828219	1856.2	0.059609569
1851.2	0.101625336	1856.4	0.172971242
1851.4	0.046919844	1856.6	0.049342754
1851.6	0.074436486	1856.8	0.04675792
1851.8	0.070184805	1857	0.0447726
1852	0.048885636	1857.2	0.054090778
1852.2	0.100901593	1857.4	0.071631637
1852.4	0.070125103	1857.6	0.067577986
1852.6	0.063857528	1857.8	0.073011396
1852.8	0.077035537	1858	0.076307758
1853	0.047905905	1858.2	0.067088322
1853.2	0.082110368	1858.4	0.054365304
1853.4	0.045594705	1858.6	0.122741754
1853.6	0.060756274	1858.8	0.041592924
1853.8	0.053926653	1859	0.035195045
1854	0.096107032	1859.2	0.035857844
1854.2	0.041260759	1859.4	0.021105667
1854.4	0.052460749	1859.6	0.006343221
1854.6	0.046770099	1859.8	0.003505614
1854.8	0.062171493	1860	0.009470676
1855	0.049859876		

FDD-LTE (1860-1875MHz), China Mobile TDD-LTE (1880-1900MHz), China Telecom CDMA (2110-2170MHz), and China Telecom TDD-LTE (2635-2655MHz).

In order to ensure that the radiation is within the limitation, we calculated the power density of each band. For the sake of clarity, we only show the calculation process for how to obtain the RF power density of China Unicom FDD-LTE band.

The power density of each single frequency point was calculated by using Equation (2), and listed in Table 3.

$$P_s(f) = \frac{P_s(\mu W)}{A_e} \tag{2}$$

where $P_s(\mu W)$ is the measured power of each single frequency point, A_e is the effective area of the antenna, which can be calculated by using equation (3):

$$\frac{G}{A_e} = \frac{4\pi}{\lambda^2} \tag{3}$$

G represents the measured gain of the antenna, and λ is the wavelength. They are both frequency dependent parameters.

Then we use the curve fitting toolbox of MATLAB to do the function fitting of the power density distribution with frequency (1850-1860MHz). The suitable function is expressed as the following fifth order Fourier fitting function (4):

$$\begin{aligned} P(f) = {} & 0.1825 - 0.1113 \times \cos(f \times 0.416) + 0.1959 \\ & \times \sin(f \times 0.416) \\ & - 0.1018 \times \cos(2 \times f \times 0.416) - 0.1567 \\ & \times \sin(2 \times f \times 0.416) \\ & + 0.1366 \times \cos(3 \times f \times 0.416) - 0.02421 \\ & \times \sin(3 \times f \times 0.416) \\ & - 0.01521 \times \cos(4 \times f \times 0.416) + 0.0716 \\ & \times \sin(4 \times f \times 0.416) \\ & - 0.02452 \times \cos(5 \times f \times 0.416) - 0.01235 \\ & \times \sin(5 \times f \times 0.416) \end{aligned} \tag{4}$$

Finally by substituting the fitting function into equation (5), we can get the calculated power density for the Unicom FDD-LTE band is $0.615 \mu W/cm^2$.

$$P(\mu W/cm^2) = \int_{f1}^{f2} P(f) df \tag{5}$$

With the same process, the measured power density for all the wireless systems in service can be achieved. And the results for all the systems are within the limitation set by ICNIRP (The international commission for non-ionizing radiation protection) [21] and IEEE [22]. The results on the other hand proved the antenna can be used for these aforementioned wireless communication bands.

V. CONCLUSION

In this paper, a compact symmetrical CPW-fed SWB antenna is proposed. By using specially designed smoothing structure in both radiation part and the notched ground, a wide band from 0.4GHz to higher than 20GHz with a bandwidth ratio larger than 50:1 can be realized. Throughout the whole band, the maximum measured gain of the antenna is 6.3dBi and the radiation efficiency changes from 30% to 96%. Below 5GHz, the antenna has a quasi omnidirectional performance. Also, the SWB antenna has been used for ambient RF radiation density measurement in the urban area of Nanjing. All radio frequency bands in service like GSM, DCS and LTE can be measured, which on the other hand proves the efficiency of the wideband performance.

REFERENCES

[1] V. Rumsey, *Frequency Independent Antennas*. New York, NY, USA: Academic, 1966.

[2] S. Barbarino and F. Consoli, "Study on super-wideband planar asymmetrical dipole antennas of circular shape," *IEEE Trans. Antennas Propag.*, vol. 58, no. 12, pp. 4074–4078, Dec. 2010.

[3] A. Azari, "A new super wideband fractal microstrip antenna," *IEEE Trans. Antennas Propag.*, vol. 59, no. 5, pp. 1724–1727, May 2011.

[4] M. A. Dorostkar, M. T. Islam, and R. Azim, "Design of a novel super wide band circular-hexagonal fractal antenna," *Prog. Electromagn. Res.*, vol. 139, pp. 229–245, Apr. 2013.

[5] V. Waladi, N. Mohammadi, Y. Zehforoosh, A. Habashi, and J. Nourinia, "A novel modified star-triangular fractal (MSTF) monopole antenna for super-wideband applications," *IEEE Antennas Wireless Propag. Lett.*, vol. 12, pp. 651–654, 2013.

[6] Y. Dong, W. Hong, L. Liu, Y. Zhang, and Z. Kuai, "Performance analysis of a printed super-wideband antenna," *Microw. Opt. Technol. Lett.*, vol. 51, no. 4, pp. 949–956, Apr. 2009.

[7] K.-R. Chen, C.-Y.-D. Sim, and J.-S. Row, "A compact monopole antenna for super wideband applications," *IEEE Antennas Wireless Propag. Lett.*, vol. 10, pp. 488–491, 2011.

[8] M. Manohar, R. S. Kshetrimayum, and A. K. Gogoi, "Printed monopole antenna with tapered feed line, feed region and patch for super wideband applications," *IET Microw., Antennas Propag.*, vol. 8, no. 1, pp. 39–45, 2014.

[9] J. Liu, K. P. Esselle, and S. G. Hay, "Study of an extremely wideband monopole antenna with triple band-notched charactersistics," *Prog. Electromagn. Res.*, vol. 123, no. 8, pp. 143–158, 2012.

[10] J. Liu, K. P. Esselle, and S. Zhong, "An asymmetrical structure for printed SWB antenna miniaturization," in *Proc. 14th Int. Symp. Antenna Technol. Appl. Electromagn. Amer. Electromagn. Conf.*, Ottawa, ON, Canada, 2010, pp. 1–4.

[11] J. Liu, K. P. Esselle, S. G. Hay, and S. S. Zhong, "Compact super-wideband asymmetric monopole antenna with dual-branch feed for bandwidth enhancement," *Electron. Lett.*, vol. 49, no. 8, pp. 515–516, Apr. 2013.

[12] J. Liu, P. E. Karu, S. G. Hay, and S. Zhong, "Achieving ratio bandwidth of vol. 25, p. 1from a printed antenna using a tapered semi-ring feed," *IEEE Antennas Wireless Propag. Lett.*, vol. 10, pp. 1333–1336, 2011.

[13] M. Alibakhshikenari, S. B. Virdee, and A. Ali, "Miniaturized planar-patch antenna based on metamaterial L-shaped unit-cells for broadband portable microwave devices and multiband wireless communication systems," *IET Microw., Antennas Propag.*, vol. 12, no. 7, pp. 1080–1086, Jun. 2018.

[14] M. Alibakhshikenari, S. B. Virdee, and H. C. See, "Wideband printed monopole antenna for application in wireless communication systems," *IET Microw., Antennas Propag.*, vol. 12, no. 7, pp. 1222–1230, Jun. 2018.

[15] M. Akbari, M. Koohestani, C. Ghobadi, and J. Nourinia, "Compact CPW-fed printed monopole antenna with superwideband performance," *Microw. Opt. Technol. Lett.*, vol. 53, no. 7, pp. 1481–1483, Jul. 2011.

[16] L. Chang, J. Q. Zhang, M. F. Zhang, J. S. Zhou, and Y. F. Wang, "A compact CPW-fed planar printed antenna with modified ground structure for super-wideband applications," in *Proc. URSI Gen. Assem. Sci. Symp. (URSI GASS)*, Beijing, China, 2014, pp. 1–4.

[17] S. S. Zhong, X. L. Liang, and W. Wang, "Compact elliptical monopole antenna with impedance bandwidth in excess of 21:1," *IEEE Trans. Antennas Propag.*, vol. 55, no. 11, pp. 3082–3085, Nov. 2007.

[18] TV. Son, K. Gina, and CH. Keum, "Planar super-wideband loop antenna with asymmetric coplanar strip feed," *Electron. Lett.*, vol. 52, no. 2, pp. 96–98, 2016.

[19] J. L. Volakis, *Antenna Engineering Handbook*. New York, NY, USA: McGraw-Hill, 2007.

[20] K. Mimis, D. R. Gibbins, S. Dumanli, and G. T. Watkins, "The ant and the elephant: Ambient RF harvesting from the uplink," *IET Microw., Antennas Propag.*, vol. 11, no. 3, pp. 386–393, 2017.
[21] International Commission on Non-Ionizing Radiation Protection, "Guidelines for limiting exposure to time-varying electric and magnetic fields (1 Hz–100 kHz)," *Health Phys.*, vol. 99, no. 6, pp. 818–836, 2010.
[22] *IEEE B E. IEEE Standard for Safety Levels With Respect to Human Exposure to Radio Frequency Electromagnetic Fields, 3 kHz to 300 GHz Amendment 1: Specifies Ceiling Limits for Induced and Contact Current, Clarifies Distinctions Between Localized Exposure and Spatial Peak Power Density*. IEEE Standard C95.1a-2010, Sep. 2010.

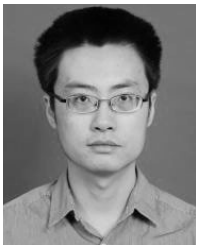

LINGSHENG YANG (Member, IEEE) received the B.S. degree from the Department of Communication Engineering, Nanjing University of Science and Technology, China, in 2001, and the M.S. and Ph.D. degrees from the Faculty of Information Science and Electrical Engineering, Kyushu University, Japan, in 2009 and 2012, respectively.

Since 2012, he has been an Assistant Professor with the Electronics and Information Engineering Department, Nanjing University of Information Science and Technology. He is the author of more than 40 articles, and more than 30 inventions. His research interests include antenna theory and design, MIMO, EMC, bioelectromagnetics, and lightning detection.

DAN ZHANG received the B.S. degree in mechanical engineering from the Dalian University of Technology, Dalian, China, in 1999, the M.S. and Ph.D. degrees in electromagnetic waves and communication engineering from Kyushu University, Fukuoka, Japan, in 2004 and 2007, respectively. He is currently a Professor of electronic and communication engineering with the College of Information Science and Technology, Nanjing Forestry University, China. In 2015, he was introduced to Nanjing Forestry University as a high-level talent. In recent years, more than 50 articles have been published by the first author, and more than ten patents have been applied for granted. He has been invited by the International Professional Society for many times to preside over international conferences or give academic speeches. His research has been focused on electromagnetic field theory, microwave and optical technology, and nondestructive testing and imaging. He is currently an Associate Editor of *IEICE Electronics Express* and a reviewer of several internationally renowned professional journals.

XIAOLEI ZHU was born in Yancheng, Jiangsu, China, in 1994. He received the B.S. degree in electronics engineering from the Chifeng College, in 2018. He is currently pursuing the master's degree with the Electronics and Information Engineering Department, Nanjing University of Information Science and Technology. His research interests include antennas and EMC.

YAJIE LI received the B.S. and M.S. degrees from the School of Medicine, Zhejiang University, China, in 2005 and 2007, respectively.

From 2007 to 2012, she was with the First Affiliated Hospital of Wenzhou Medical University. Since 2012, she has been an Attending Doctor with the Geriatric Department, Zhongda Hospital, Southeast University. She is an author of nearly 20 articles. Her research interests include gerontology, internal medicine of digesting, medical engineering, and bioelectromagnetics.